

Edward E. Osakue

Department of Industrial Technology
Texas Southern University
Houston, Texas,
USA

Lucky Anetor

Department of Engineering
Texas Southern University
Houston, Texas,
USA

Kendall Harris

Provost & Vice President
for Academic Affairs
Texas Southern University
Houston, Texas,
USA

A Parametric Study of Frictional Load Influence in Spur Gear Bending Resistance

A revised Lewis bending fatigue stress capacity model for spur gears is presented and used to study the influence of mesh friction on root stress. It took the original Lewis formula and made modifications for dynamic loads, shear stress, and mesh friction in spur gear design. The study reveals that mesh friction may increase bending stress by up to 6% in enclosed cylindrical gear drives when an average mesh friction coefficient of 0.07 is assumed. A possible increase of 15% in root stress may occur in open gear drives when the mesh friction coefficient is taken as 0.15, a value considered to be representative for properly maintained open drives. To account for mesh frictional load and other factors directly influencing mesh friction, a friction load factor of 1.1 is suggested and introduced to gear service load estimation for enclosed gear drives and 1.15 for open gear drives.

Keywords: Lewis form factor, Mesh friction factor, Root bending stress

1. INTRODUCTION

A gear is a toothed disk used to transmit power and motion when mounted on a rotating shaft. In most applications, the gear is made separate from the shaft but could be made integral with it, especially when the gear is small in size. Spur gears have tooth profile projecting radially with the gear width parallel to the axis of the shaft and they have been used since ancient times [1].

The resistance of gear teeth to failure in bending is called beam strength and gear failure in bending fatigue is a common problem [2, 3, 4]. Fatigue failure is due to crack formation and propagation induced by repeated loading. A crack normally initiates at a discontinuity where there is a cyclic maximum stress [5, 6]. Cracks grow along planes normal to the maximum tensile stress [5] and when the growth becomes unstable, brittle fracture rapidly follows. Through hardened gears most often fail in bending fatigue due to a crack initiated at the surface in the root area. Because the surface hardness of case-hardened gears is higher than the core value, the bending fatigue strength of the gear root surface can be higher than that of the core. Therefore, bending fatigue failure may occur at the transition zone between case-hardness and core-hardness if the induced stress at the junction is more than the available core fatigue strength [7]. In fact, case-hardened gears generally fail in fatigue at the boundary of case-core hardness, except when there is sharp stress raiser at the surface [8].

In 1892, Lewis modeled a gear tooth in bending as a short cantilever beam on a rigid base with the transmitted load applied near the tip of the gear tooth [5, 6]. The maximum tensile stress occurs at the root radius

on the loaded or active side of the gear tooth. Due to repeated loading of a gear tooth, this region becomes the preferential site for the initiation of fatigue crack. This beam model still serves as the basis for gear bending fatigue design today. Consequently, various gear bending capacity standards, such as those of the International Standardization Organization (ISO), American Gear Manufacturers Association (AGMA), and Japanese Industrial Standards (JIS) are modifications of the Lewis formula.

Mesh friction is the friction occurring in the contact zone between the teeth of a gearset in a mesh. AGMA gear standards recognize the fact that gear surface finish may affect the quality of contact. Surface finish in gears may be influenced by cutting, shaving, lapping, grinding, and shot-peening, etc. [7, 9]. In AGMA model, a surface finish factor may be assumed and given a value of unity for gears made with conventional methods but can be given a value above unity for unusually rough surface finish or for known presence of detrimental residual stresses [7]. However, this factor is not directly linked with friction.

Gear mesh friction is complicated with contributions from sliding and rolling. However, rolling motion occurs only in the vicinity of the pitch point, while mixed sliding and rolling motions occur elsewhere. Higher peripheral speed facilitates the formation of an oil wedge in the contact area, resulting in lower frictional losses [10]. For enclosed gear drives, mesh friction is in the range of 0.04 to 0.10 [8, 9, 10, 11, 12] and Maitra [11] suggests an average value of 0.07. Open gear drives operate in much harsher environments than enclosed gear drives and lubrication is not as good or effective as in enclosed gears. Higher friction is therefore expected, since they operate mostly in boundary to dry friction regimes. For instance, the coefficient of friction in boundary lubrication is in the range of 0.05 to 0.15 [9]. Friction is a poorly behaved phenomenon, being influenced by many factors; including surface finish, wear resistance, temperature, humidity, contamination, lubricant, and sliding speed. Because of stick-slip behavior and wide

Received: October 2019, Accepted: December 2019

Correspondence to Prof. Edward E. Osakue
Department of Industrial Technology, Texas
Southern University, Houston, Texas, USA
Email: edward.osakue@tsu.edu

doi:10.5937/fme20022940

© Faculty of Mechanical Engineering, Belgrade. All rights reserved

FME Transactions (2020) 48, 294-306 294

variation in friction coefficient values, frictional behavior is very unpredictable [13, 14]. Mesh friction has the detrimental effect of promoting the formation of cyclic tensile stress component in the contact zone which enhances fatigue crack propagation [15] and also reducing power transmission efficiency.

Li and Mao [16] developed a numerical method for the study of the influence of mesh friction on the contact force, bending stress, and transmission error in spur gears. They concluded that frictional force should not be ignored in gearing because it increases the bending stress and transmission error. Increased transmission error generally translates into increased vibrations and noise which can further increase the contact force. Eng et al [17] investigated frictional stress analysis of spur gears with misalignments using finite element method. The mesh friction coefficient was varied from 0.1 to 0.3 in values while the contact and bending stresses were estimated. They found that the contact stress increased by 5 to 6% while the bending stress increased by 4.6% for a mesh friction value of 0.3. Thus there appears to be no analytical solution method or model for the influence of frictional load on spur gear bending stress. Generally, analytical solutions are faster and less costly to implement programmatically in software development.

This study investigates the influence of mesh friction on the bending stress of spur gears parametrically. The influence is explored by decomposing the frictional load into tangential and radial frictional load components. It is demonstrated that mesh friction slightly increases the effect of the nominal transmitted load, thus resulting in higher bending stresses than expected when mesh friction is ignored. Specifically, it is shown that the tangential frictional load contributes more than the radial frictional load in the increase in bending stress. Consequently, it may be justified to *always* account for the increase in bending stress due to mesh friction. Hence, it is suggested that a frictional load factor component may be included in the service load factor estimate in spur gear design in particular, and in gear design in general.

2. MESH FRICTIONAL LOAD COMPONENTS

The torque and tangential force loads on a gear tooth are:

$$T_1 = \frac{30P_1 \times 10^3}{\pi N_1} \quad F_t = \frac{2T_1 \times 10^3}{d_1} \quad (1)$$

Equation (1) has two entries and should be interpreted as Eq. (1a) and Eq. (1b) from left to right. The same rule should be applied to other equations of similar nature.

The radial and normal forces on spur gears are given in Eq. (2).

$$F_r = F_t \tan \varphi_t \quad F_n = \frac{F_t}{\cos \varphi_t} \quad (2)$$

The gear tip contact angle at the beginning of meshing is given in Eq. (3).

$$\varphi_a = \cos^{-1} \left(\frac{r_p \cos \varphi_t}{r_a} \right) = \cos^{-1} \left(\frac{z \cos \varphi_t}{z+2} \right) \quad (3)$$

In Fig. 1, we consider a spur gear that is loaded in bending by a force at the tip of the gear tooth. The friction force f_n results from the presence of mesh friction and is assumed to act at the contact angle shown. This will be the point where the relative sliding velocity is highest at the beginning of a mesh. The exit point at the dedendum radius is another point of high relative sliding velocity. The contact at the tip of the gear occurs at point A, but the effective moment arm is determined by the projection of point A onto the centerline of the tooth profile at point B. Since the contact point moves downward, the friction force would point upward to oppose the motion.

The frictional forces are:

$$f_n = \zeta_m F_n \quad f_t = f_n \sin \varphi_a \quad f_r = f_n \cos \varphi_a \quad (4)$$

The bending force on the gear tooth is:

$$F_t' = F_t + f_t \quad F_t' = \alpha_t F_t \quad \alpha_t = 1 + \frac{\zeta_m \sin \varphi_a}{\cos \varphi_t} \quad (5)$$

Eq. (5c) indicates that the presence of friction increases the tangential bending load on a gear tooth, since α_t is greater than unity. Hence at the tip of the gear, the load carried by a pair of meshing gears will be more than the nominal transmitted load. The implication of this is that the bending moment at the root of the gear is slightly increased.

The compressive force on the gear tooth is:

$$F_r' = F_r - f_r \quad F_t' = \alpha_r F_t \tan \varphi_t \quad \alpha_r = 1 - \frac{\zeta_m \cos \varphi_a}{\sin \varphi_t} \quad (6)$$

Eq. (6c) shows that the radial compressive load is reduced by the presence of friction in the mesh, since α_r is less than unity. Therefore, the beneficial effect of the radial load in reducing the tensile stress at the gear root is slightly over estimated when friction is neglected. From Eqs. (5c) and (6c), it is clear that the resultant tensile stress is actually slightly higher in spur gear when mesh friction is not ignored. Mesh friction in cylindrical gear drives is considered in Appendix A1.

Fig. 2 to Fig. 7 show the plots of the friction load factors against the gear tip contact angle for 20° standard tooth profile for spur gears when the mesh friction coefficients of 0.02, 0.05, 0.07, 0.10, 0.15 and 0.20; are assumed respectively. The upper curves in these figures show the tangential frictional load factor while the lower curves show the radial frictional load factor. The tangential frictional load factor is highest for small numbers of gear teeth when the tip contact angle is largest. The radial frictional load factor is lowest for high numbers of gear teeth when the tip contact angle is smallest. Note that higher values of the tangential frictional load factor result in higher root bending stresses while lower values of the radial load factor result in higher root bending stresses. Therefore, the worst load combination would occur at these situations, but they are however, mutually exclusive in practice for a single gear tooth. Theoretically, they give the limit conditions and thus the most conservative in frictional load influence in the bending resistance of spur gears.

Figs 2 to 5 cover the range of mesh friction coefficient for enclosed cylindrical gear drives while Figs. 5 to 7 may be considered as representing the range for open cylindrical gear drives that are properly maintained in operation. Poorly maintained open drives are likely to operate in dry friction regime so that higher friction coefficients above 0.20 may be expected. In Figs. 2 to 7, gears with smaller number of teeth or higher tip contact angles experience higher tangential frictional load.

However, gears of smaller number of teeth or higher tip contact angles experience lower radial load reduction and benefit more from the influence of the radial compressive stress is reduced by mesh friction. Consequently, gears with lower number of teeth experience higher compressive stresses due to the presence of friction in a gear mesh.

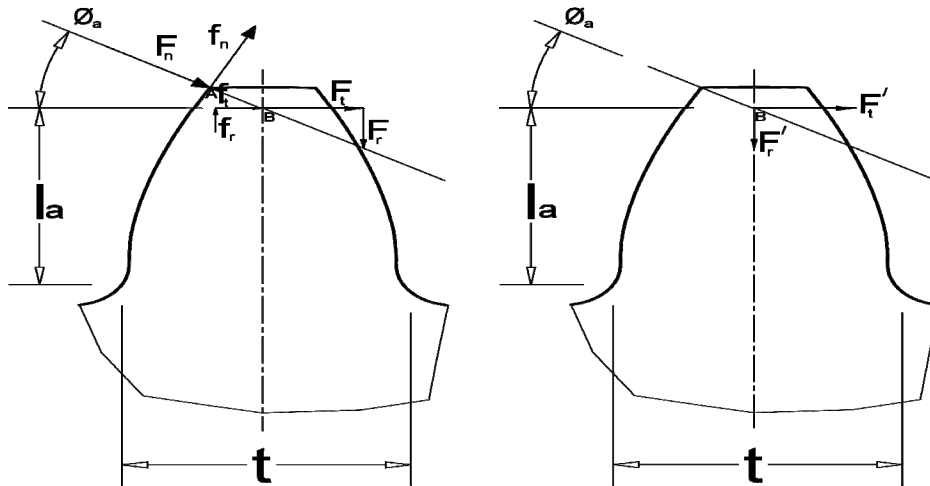


Fig. 1: Bending forces on spur gear tooth

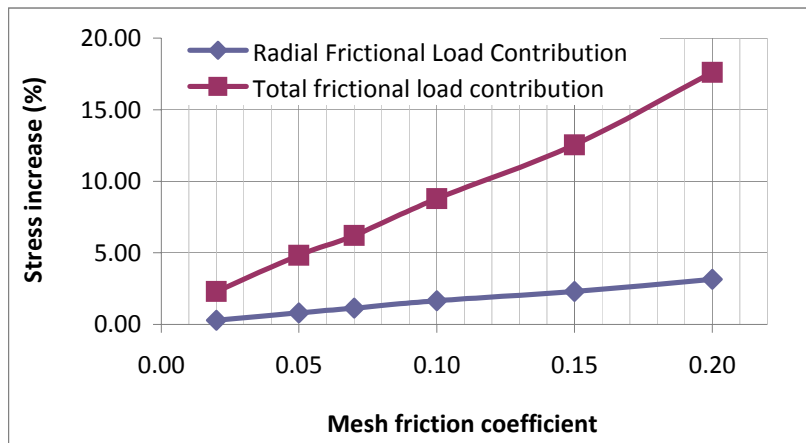


Fig. 2: Frictional load factors for 0.02 coefficient

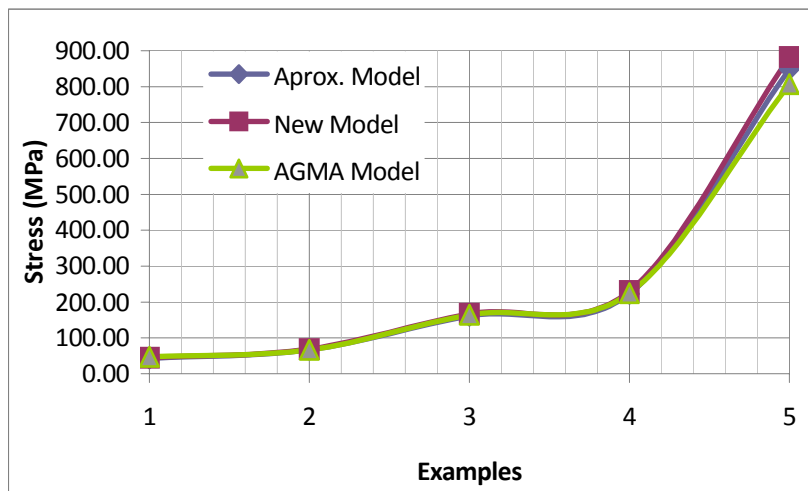


Fig. 3: Frictional load factors for 0.05 coefficient

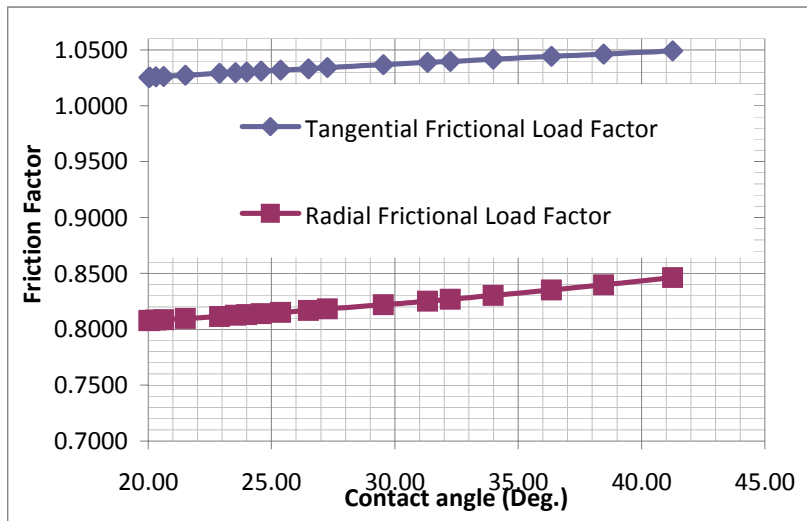


Fig. 4: Frictional load factors for 0.07 coefficient

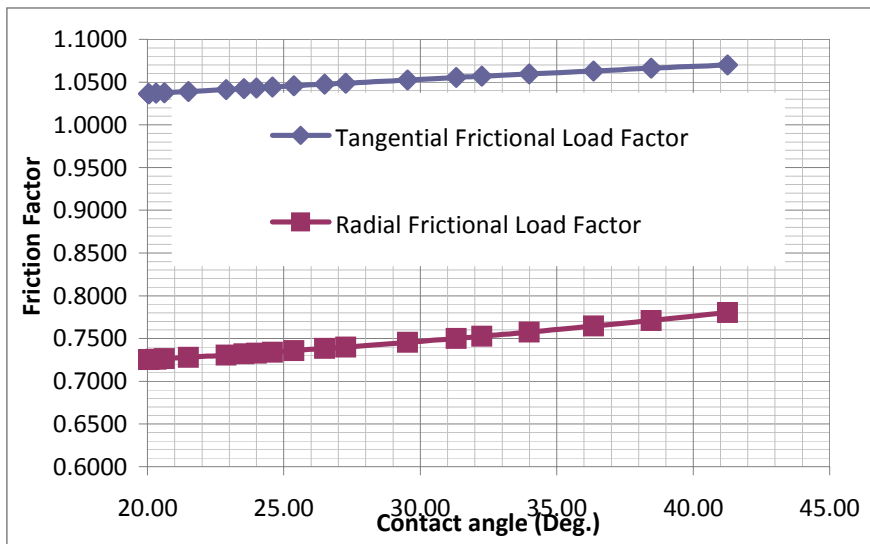


Fig. 5: Frictional load factors for 0.10 coefficient

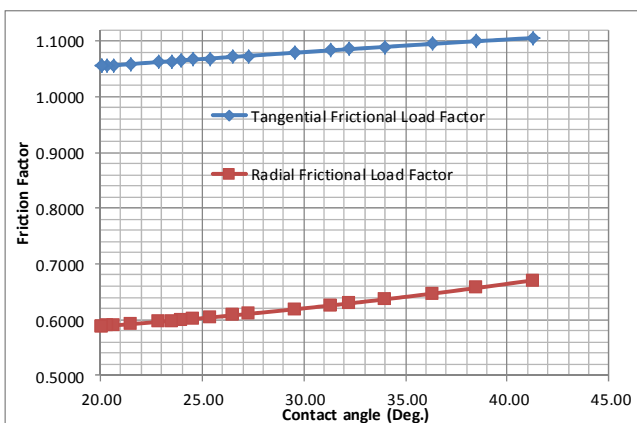


Fig. 6: Frictional load factors for 0.15 coefficient

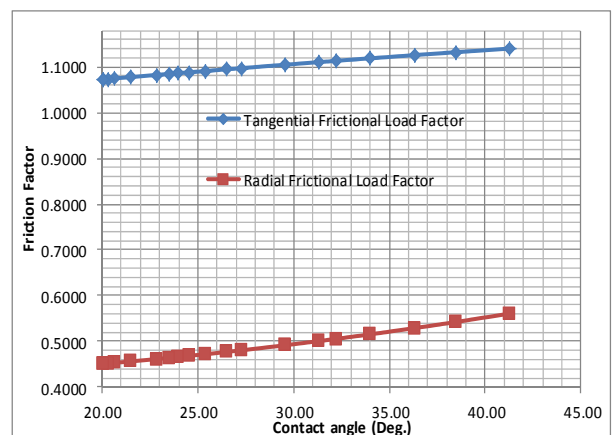


Fig. 7: Frictional load factors for 0.20 coefficient

Table 1 is the summary of Fig. 2 to Fig. 7 in which column 1 of the table shows the mesh friction values, column 2 shows the tangential friction factor values and column 3 shows the radial friction factor values. Due to the nebulous nature of friction and high variability of

friction coefficient values, a conservative approach is adopted in populating columns 2 and 3 of Table 1. Maximum values of the tangential friction factor values were read from Fig. 2 to Fig. 7 while minimum values of the radial friction factors were read. However, these

values correspond to opposite ends in the plots: the tangential friction factor corresponds to low number of teeth while the radial friction factor corresponds to higher number of teeth in a gear. Such an approach is predicated on the very high variability that is associated with friction coefficient values. The tangential friction factor values in column 2 of Table 1 give the possible increase in the tangential force as a result of the mesh friction value indicated in column 1. These values directly translate to increases in the root bending stress of a gear tooth. For instance, a mesh friction coefficient of 0.07 leads to a 5% increase in the root bending stress. The radial friction factor values in column 3 of Table 1 give the possible proportion of the radial load that produces a compressive stress at the gear tooth root. The difference between unity and the values indicated in column 3 is the proportion of the radial load that leads to further increase in the root bending stress due to the friction in the contact mesh. How much that increase is, cannot be determined directly from the radial friction factor as it is with the tangential friction factor. Further study is required therefore, to estimate the numerical increases that can result from the radial frictional load component. Consequently, the Lewis bending stress formula will be used for investigating the contributions of the radial frictional load to increases in root bending stress because it can be modified to accommodate frictional load.

Table 1: Summary of Mesh Friction Factors

Mesh Friction Coefficient	Tangential Friction Factor	Radial Friction Factor
0.02	1.02	0.95
0.05	1.04	0.86
0.07	1.05	0.80
0.10	1.07	0.71
0.15	1.10	0.60
0.20	1.14	0.45

3. MODIFIED LEWIS BENDING CAPACITY MODEL FOR SPUR GEARS

When load shearing and static load are assumed, the Lewis bending stress formula may be expressed as:

$$\sigma_{bt} = \frac{F_t}{\varpi_t b m_t Y'} \quad (7)$$

Eq. (7) is evaluated separately for the pinion and gear in gear design. The pinion is usually more vulnerable to bending stress failure, being of a smaller root tooth thickness. Eq. (8a) gives the expression for the modified Lewis bending stress form factor when the radial compressive stress is considered [10, 18] without friction in the gear mesh. Thus, if the radial compressive force is neglected as assumed by Lewis, the Eq. (8b) is obtained.

$$Y = \frac{1}{\left(\frac{\cos \varphi_a}{\cos \varphi_t} \right) \left[\frac{6l_a}{t} - \tan \varphi_a \right] \frac{m_t}{t}} \quad (8a)$$

$$Y' = \frac{1}{\left(\frac{\cos \varphi_a}{\cos \varphi_t} \right) \left[\frac{6l_a}{t} \right] \frac{m_t}{t}} \quad (8b)$$

It is clear that Eq. (8a) will always give higher values compared to Eq. (8b) because of the compressive stress considered and the result is a lower bending stress. This explains why the value of Y for modern gear standards that account for the compressive radial force is slightly higher than Y' . Note that Y or Y' values for the pinion and gear can be estimated from a single curve.

3.1 Direct Compressive Stress

The radial force induces a compressive stress which is given in Eq. (9a). Eq. (9b) is obtained by combining Eq. (7) and Eq. (9a).

$$\sigma_{cr} = \frac{F_r'}{\varpi_t b t} = \frac{\alpha_r F_t \tan \varphi_t}{\varpi_t b t} \quad (9a)$$

$$\sigma_{cr} = \frac{\sigma_{bt} \alpha_r m_t Y' \tan \varphi_t}{t} \quad (9b)$$

The resultant bending stress at the gear root is:

$$\sigma_b = \sigma_{bt} - \sigma_{cr} \quad (10a)$$

$$\sigma_b = \sigma_{bt} \left(1 - \alpha_r Y' \tan \varphi_t \frac{m_t}{t} \right) \quad (10b)$$

3.2 Direct Shear Stresses

The transverse force also induces direct shear stress on the gear which is:

$$\tau_s = \frac{F_t}{\varpi_t b t} \quad \tau_s = \sigma_{bt} Y' \frac{m_t}{t} \quad (11)$$

3.3 Equivalent Root Tensile Stress

The equivalent tensile stress at the gear root may be based on distortion energy theory or maximum shear stress theory depending on whether the material is ductile or brittle [7, 11]. Most gears are made from ductile materials, so the equivalent tensile stress at the tooth root may be estimated by applying the distortion energy theory. For a plane stress situation, the equivalent tensile stress based on the distortion energy theory is:

$$\sigma_t = \sqrt{\sigma_b^2 + 3\tau_s^2} \quad (12)$$

The dedendum circle is generally connected with the involute profile of a gear tooth with a fillet. This introduces a geometric discontinuity at the gear root resulting in stress concentration. Stress concentration was not known in the days of Lewis; but it is very important today because experimental and simulated results indicate that it can significantly increase local stresses [19]. Therefore, a stress concentration factor should be included in the Lewis formula for it to be more realistic.

Since there are both normal and shear stresses, Eq. (12) may be modified as:

$$\sigma_t = \sqrt{k_\sigma^2 \sigma_b^2 + 3k_\tau^2 \tau_s^2} \quad (13)$$

On substituting Eq. (10b) and Eq. (11b) into Eq. (13) and simplifying, we get:

$$\sigma_t = \frac{F_t k_\sigma k_t'}{b m_t Y' \varpi_t} \quad \sigma_t = \frac{2k_\sigma k_t' T \times 10^3}{d b m_t Y' \varpi_t} \quad (14)$$

where:

$$k_t' = \sqrt{\left(1 - \frac{\alpha_r m_t Y'}{t} \tan \phi_t\right)^2 + 3 \left[\frac{Y' m_t k_\tau}{k_\sigma t}\right]^2} \quad (15)$$

It can be shown that:

$$t = m_t \kappa \quad \kappa = \sqrt{6 \lambda_a Y'} \quad (16)$$

Appendix A2 describes a method for estimating λ_a using the rack tooth profile.

Substitute Eq. (16a) into Eq. (15) to obtain Eq. (17) as:

$$k_t' = \sqrt{\left(1 - \frac{\alpha_r Y'}{\kappa} \tan \phi_t\right)^2 + 3 \left[\frac{Y' k_\tau}{\kappa k_\sigma}\right]^2} \quad (17)$$

Apparently, the mesh friction can only be estimated after a gearset dimensions are established and a lubricant is chosen. Please refer to Appendix A1. Therefore, the value of the tangential and radial frictional load factors cannot be established at the beginning of a design when the mesh friction coefficient is unknown. As a simplification, it is reasonable to ignore the radial frictional load influence by assuming a value of unity for the radial frictional load factor. Hence Eq. (17) can be modified as:

$$k_t = \sqrt{\left(1 - \frac{Y'}{\kappa} \tan \phi_t\right)^2 + 3 \left[\frac{Y' k_\tau}{\kappa k_\sigma}\right]^2} \quad (18)$$

Values of stress concentrations are required in Eqs. (14), (17) and (18). Table 2 is suggested for use in gear bending stress estimation during initial sizing [20]. The values of the stress concentration factors in the table have no relationship with the point of load application on a gear tooth.

Table 2: Stress Concentration Factors for Gears

Gear Material Type	k_σ	k_τ
Cast iron and non-ferrous materials	1.40	1.75
Normalized steels (< 300 HVN)	1.50	1.85
Quenched & tempered steels (≤ 450 HVN)	1.60	2.00
Case-hardened steels (> 450 HVN)	1.50	1.85

4. SERVICE LOAD FACTOR (K_s)

The original Lewis formula assumes the gear load to be static but it is dynamic in practice and experience shows that the forces acting on equipment in service are generally higher than the rated or nominal values in gear drives. Practically, the design or service load is often estimated by multiplying the rated load with a service load factor which is used to account for load increases during normal operations of gearsets. It is a load magnification factor in gear design.

In the AGMA model without friction consideration:

$$K_{ss} = K_a K_v K_m K_r \quad (19)$$

When tangential frictional load is accounted for:

$$K_s' = \alpha_t K_{ss} \quad (20)$$

For an approximate analysis with both tangential and radial frictional load components accounted for:

$$K_s = K_{ss} K_o \quad K_o > \alpha_t a \quad (21)$$

5. WORKING VERSIONS OF MODIFIED LEWIS BENDING STRESS FORMULA

Surface roughness can influence friction, especially rough surfaces, but it seems to have a greater influence on the actual contact area when two bodies are in relative sliding motion [21]. So, the effect of surface roughness may be accounted for through an effective facewidth factor (λ_e). Other factors such as thermal gradient, centrifugal forces, work hardening, residual stresses [7], etc. can distort pinion or gear shape and lead to teeth mismatch so that full contact does not occur over the nominal facewidth of meshing gears. In general, the effective facewidth factor will be assumed to account for surface roughness, surface treatment quality and miscellaneous effects that make contact over the full nominal facewidth of a gear impossible. AGMA [22] suggests a value of 0.95 for the effective facewidth factor of helical gears; this value is here adopted for spur gears also. Eq. (14) can then be modified by introducing the service load factor and the effective facewidth factor. Equations (22) to (25) are derived from Eq. (14) with the service load factor and the effective facewidth factor incorporated.

When mesh friction is neglected, both tangential and radial frictional load factors are ignored. The root stress can be calculated as:

$$\sigma_t = \frac{2k_\sigma k_t K_{ss} T \times 10^3}{\lambda_e \varpi_t m_t b d Y'} \quad (22)$$

Eq. (22) is required to verify that the new approach presented is reasonable as the stress estimates from it can be compared with current AGMA model that does not consider frictional load contribution to root stress.

When radial frictional load factor is unity:

$$\sigma_t = \frac{2k_\sigma k_t K_s' T \times 10^3}{\lambda_e \varpi_t m_t b d Y'} \quad (23)$$

The modified Lewis model which takes both tangential and radial frictional load factors into account is:

$$\sigma_t = \frac{2k_\sigma k_t' K_s' T \times 10^3}{\lambda_e \varpi_t m_t b d Y'} \quad (24)$$

Note that Eq. (24) and Eq. (17) constitute the revised Lewis bending stress capacity model. The effective stress increase due to the radial frictional load factor can be assessed by comparing results of root bending stress computations from Eq. (23) with those from Eq. (24).

An approximate model that is an alternative to Eq. (24) which directly accounts for both tangential and radial frictional load through a friction load factor is:

$$\sigma_t = \frac{2k_\sigma k_t K_s T \times 10^3}{\lambda_e \varpi_t m_t b d Y'} \quad (25)$$

The difference between Eq. (24) and Eq. (25) is that the tangential and radial frictional load factors are eliminated in the latter. This is advantageous because there is no longer need to know the mesh friction coefficient since this is taken care of by the friction load factor component in the service load factor. Usually, the mesh friction coefficient can only be estimated after a gearset is sized, gearbox is designed, and a lubricant chosen. Hence using Eq. (25) as an approximation in estimating the bending stress of spur gears circumvents these other activities.

6. AGMA MODELS

The current AGMA [22] bending stress capacity model for spur gears which does not consider mesh friction always may be expressed as:

$$\sigma_{bt} = \frac{K_{ss} F_t}{b m_t J} \quad (26)$$

A slightly modified AGMA bending stress capacity model for spur gears which considers mesh friction always may be expressed as:

$$\sigma_{bt} = \frac{K_s F_t}{b m_t J} \quad (27)$$

For a proof of the validity of the revised Lewis model, results of root bending stress computations from Eq. (22) can be compared with those from AGMA model of Eq. (26) since both ignore frictional load. A good comparison should be persuasive in accepting the revised Lewis model as adequate for root bending stress estimation because AGMA standards are commonly used for gear business transactions globally.

7. DESIGN EXAMPLES

The new design formulas presented in the previous sections are applied to five design examples taken from the references stated. The equations presented were coded in Microsoft Excel for computational efficiency. The problem statements in the design examples were paraphrased and the design parameters were converted

to metric units where necessary by the authors. The goal is to estimate the root bending stresses using the new formulas and make comparisons with those from AGMA model. AGMA standards are perhaps the most popular gear standards in use and have a good reputation amongst gear designers and manufacturers.

8. DESIGN PROBLEMS

The five design problems are considered below. The solutions to the problems are available from the stated references and comparisons will be made with the estimates from the formulas presented in the sections above.

Example 1: A gearset transmits 3 kW from an electric motor with the pinion running at 1800 rpm. The gearset has a pressure angle of 20°, pinion teeth of 17, gear teeth of 52, module of 2.54 mm and facewidth of 38.1 mm [7]. Determine the root bending stress on the pinion.

Example 2: A gearset transmits 3 kW from an electric motor with the pinion running at 1425 rpm. The gearset has a pressure angle of 20°, pinion teeth of 18, gear teeth of 50, module of 2.50 mm and facewidth of 30 mm [23]. Determine the root bending stress on the pinion.

Example 3: A gearset transmits 15 kW from a pinion at 1260.5 rpm. The gearset has a module of 1.25 mm, pinion teeth of 54, gear teeth of 270, and a facewidth of 60 mm [4]. What is the expected root bending stress?

Example 4: A gearset transmits 18.64 kW from a pinion at 1750 rpm. The gearset has a module of 3.175 mm, pinion teeth of 20, gear teeth of 70, and a facewidth of 38.1 mm [1]. What is the expected root bending stress?

Example 5: A spur gearset of steel and ductile cast iron transmits a torque of 1694.8 Nm at the pinion at 406 rpm. The gearset basic size data are: 20, 127 mm, 25.4 mm. The gearset has a pressure angle of 20° [24]. What is the expected root bending stress?

9. SOLUTIONS TO PROBLEMS

Table 3 summarizes the basic gearset dimensions and load data for examples 1 to 5. The service load factors were evaluated and used for root bending stress estimation. Table 4 shows the stresses from the “no friction” revised Lewis model (Eq. (18) and Eq. (22)) and current AGMA model (Eq. (26)). Table 5 gives the results for the problems for the revised Lewis model summarized by Eq. (22), Eq. (23) and Eq. (24). Table 6 shows the increases in root bending stress from radial frictional load component and total frictional load (combined tangential and radial frictional load components). The stress concentration factor values used in the bending stress estimations were taken from Table 2 with a value of 1.5 used for bending stress and 1.85 used for shear stress.

10. DISCUSSIONS

Mesh friction can be associated with three main lubrication regimes in gearing. These are hydrodynamic, elastohydrodynamic, and boundary lubrications. In hydrodynamic lubrication, gear surfaces in relative motion

are separated by a thick oil film and it is often called thick film lubrication. In elastohydrodynamic lubrication, gear surfaces are separated by an oil film as in hydrodynamic but the oil film is thin, so it is also called thin film lubrication. Hydrodynamic lubrication is the lubrication of surfaces separated by a thick fluid film that is created by the internal pressure developed as a result of the relative motion between two non-parallel surfaces. In gearing, this lubrication type is expected at high speed and low to moderate contact stresses. Elastohydrodynamic lubrication (EHL) is a thin fluid-film lubrication in which hydrodynamic action is significantly enhanced by surface elastic deformation and lubricant viscosity increases due to high contact pressure. This type of lubrication is expected at high speed and high contact stress. The frictional resistance in full film lubrication arises from the viscosity of the lubricant and is usually very low. Consequently frictional damage is minima and occurs mainly at startup and shutdown of the gear drives. Slow turning and/or heavily loaded gear drives tend toward boundary lubrication where point loading can result in surface separation between gear teeth that is equal to or less than the mean surface roughness of the mating gears (boundary lubrication). Contact of some asperities on the gear surfaces is inevitable and frictional resistance tends to be high. Frictional damage is important in boundary lubrication

and more so in dry rubbing surfaces. Mesh friction is important because frictional work leads to heat generation which reduces both the viscosity of gear lubricants and lubrication effectiveness. Lubricant breakdown can occur if the viscosity becomes too low, resulting in severe pitting or scoring of gear surfaces. The influence of frictional load on contact and bending stresses in gear meshes makes mesh friction a relevant concern in gear drives.

Table 4 shows the results from Eq. (22) for the revised Lewis model without mesh friction consideration and Eq. (26) for AGMA current model that does not consider mesh friction also in the second and third columns, respectively. The percentage deviations in the second column from those in the third column are given in the fourth column. Fig. 8 shows the plot of the root bending stresses for visual comparison. It is seen from the deviations in Table 4 and Fig. 8 that the new revised Lewis model without mesh friction compares excellently with the current AGMA model that ignores mesh friction. Specifically, the fourth column of Table 4 indicates that the deviations are generally positive which means the stresses from the revised Lewis model are slightly higher than those of AGMA. This is expected since the new revised Lewis model considers shear stress contribution, which is ignored by the AGMA model.

Table 3: Input Parameters for Bending Stress for Examples

Parameters	Examples				
	1	2	3	4	5
Transmitted power (kW)	3	3	15	18.64	72.06
Pinion speed (rpm)	1800	1425	1260.5	1750	406
Pinion torque (Nm)	15.92	20.10	113.64	101.71	1694.8
Speed ratio	3.061	2.778	5.0	3.50	1.0
Normal pressure angle (°)	20	20	20	20	20
Normal module (mm)	2.54	2.50	1.25	3.175	6.35
Pinion teeth number	17	18	54	20	20
Gear teeth number	52	50	270	70	20
Pinion pitch diameter (mm)	43.18	45	67.5	63.5	127
Gear pitch diameter (mm)	132.08	125	337.5	222.25	127
Face width (mm)	38.1	30	60	38.1	25.4

Table 4: Results for No Friction for AGMA and New Models

Example	New Model (No Friction)	Current AGMA	Deviation (%)
Ref. [7]	40.22	42.66	-5.71
Ref. [21]	62.73	60.39	3.87
Ref. [4]	151.85	149.21	1.77
Ref. [1]	209.78	204.61	2.53
Ref. [22]	799.73	732.11	9.24

Table 5: Closed Drive Frictional Load Contributions for 0.07 Mesh friction Coefficient

Example	Friction Ignored	Radial Friction Ignored	New Model	Radial Contr. (%)	Total Friction Contr (%)
Ref. [7]	40.22	42.23	42.71	1.13	6.18
Ref. [21]	62.73	65.86	66.59	1.10	6.16
Ref. [4]	151.85	159.44	161.44	1.25	6.31
Ref. [1]	209.78	220.27	222.75	1.13	6.18
Ref. [22]	799.73	839.72	849.18	1.13	6.18
Average				1.15	6.20

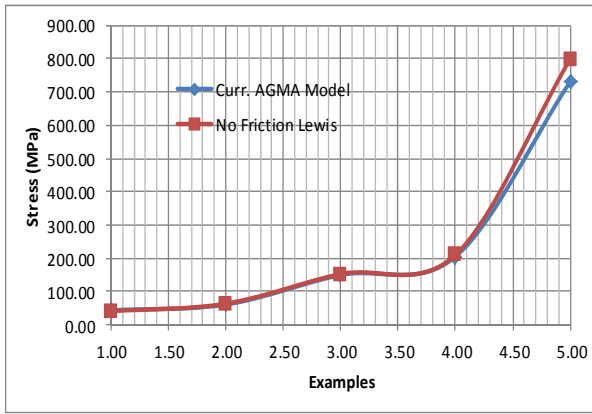


Fig. 8: New Model Verification

In order to generate the data of Table 5, root bending stresses were calculated using Eqs. (22), (23), and (24) for a mesh friction coefficient of 0.07. The second column shows the results without mesh friction being considered (Eq. (22)), the third column shows the results with only tangential frictional load (no radial frictional load) considered (Eq. (23)) and the fourth column shows the results when both tangential and radial frictional loads are considered (Eq. (24)). The percentage differences between the fourth and third columns are shown in the fifth column as the contribution of the radial frictional load component.

Table 6: Frictional Load Impact on Root Bending Stress

Mesh Friction Coefficient	Radial Contribution (%)	Total Contribution (%)
0.02	0.29	2.29
0.05	0.80	4.84
0.07	1.15	6.20
0.10	1.66	8.78
0.15	2.30	12.53
0.20	3.16	17.60

In Table 5, the percentage differences between the fourth and second columns are shown in the sixth column as the combined or total contribution of both the tangential and the radial frictional load components. The last row of the table shows the average percentage contribution to root bending stress increases by the radial frictional load component and combined tangential and radial frictional load components. Similar calculations were carried out for mesh friction coefficients of 0.02, 0.05, 0.10, 0.15, and 0.20 but the results are not presented for the sake of brevity.

Table 6 is the summary of the average percentage contribution to root bending stress increases by the radial frictional load component and combined tangential and radial frictional load components for mesh friction coefficients of 0.02, 0.05, 0.10, 0.15, and 0.20. These were obtained using the procedure described above for Table 5. It is observed that as the mesh friction coefficient increases, so does the radial frictional load contribution and similarly, the combined frictional load as expected.

Fig. 9 shows the plots of Table 6 values, where the frictional load contributions to root bending stress increases can be visualized.

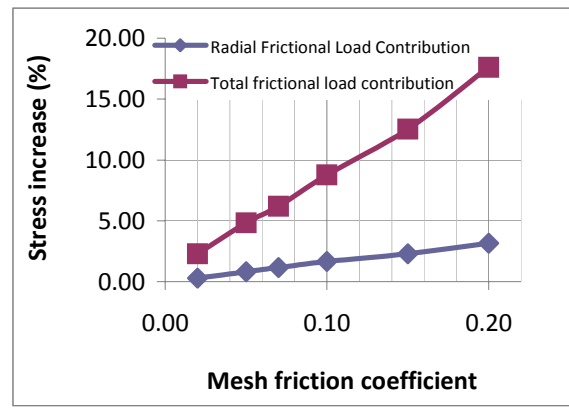


Fig. 9: Root stress increase due to mesh friction

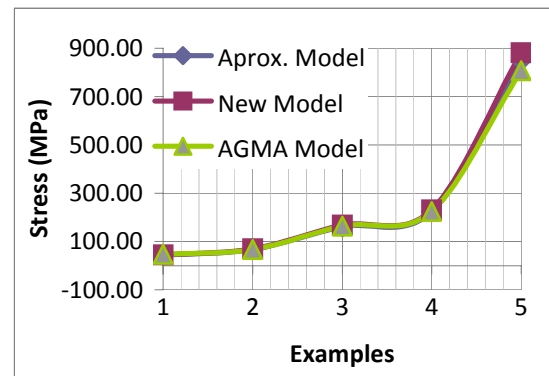


Fig. 10: Enclosed drive sample

Fig. 10 shows the graphical comparison of results obtained from Eq. (24), the new revised Lewis model, Eq. (25), the approximate model which is the alternative to Eq. (24), and Eq. (27), the adjusted AGMA model for a mesh friction coefficient of 0.07, the average value for enclosed gear drives. A friction load factor of 1.10 was used in applying Eq. (25) and Eq. (27). This figure shows very good comparison between these three models. However, the approximate model is seen to be very slightly conservative compared to the new revised Lewis model while the adjusted AGMA model gives values also very slightly lower than the new revised Lewis model. As pointed out before, it is expected that the new revised Lewis model predicts somewhat higher values of root bending stress because it accounts for shear stress which the AGMA does not. Fig. 11 is similar to Fig. 10 which shows the graphical comparison of results for a mesh friction coefficient of 0.15 that is considered representative of open gear drives. A friction load factor of 1.15 was used in applying Eq. (25) and Eq. (27) in Fig. 11.

Fig. 12 shows the graphical comparison of current AGMA model (Eq. (26)) with the new revised Lewis model (Eq. (24)), for the representative enclosed and open gear drives. This figure is intended to reveal the deviations between the current AGMA model and the new models developed in this study. The average percentage deviation between the new revised Lewis model and the current AGMA model for enclosed gear drives is 5.95%. A friction load factor 1.10 was very slightly conservative for this situation in the approximate model of Eq. (25). The average percentage

deviation between the new revised Lewis model and the current AGMA model for open gear drives is 15.16%. A friction load factor 1.15 was very slightly conservative for this situation in the approximate model of Eq. (25). The deviations from the current AGMA model in the figure indicate that mesh friction can have significant impact on the root bending stress in spur gears. Consequently, it will be reasonable to always consider mesh friction in root stress estimation in gear design.

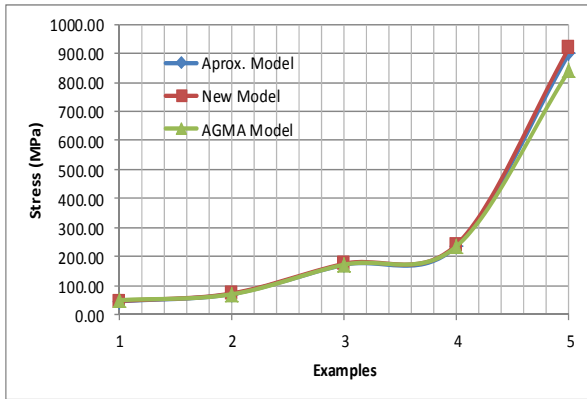


Fig. 11: Open drive sample

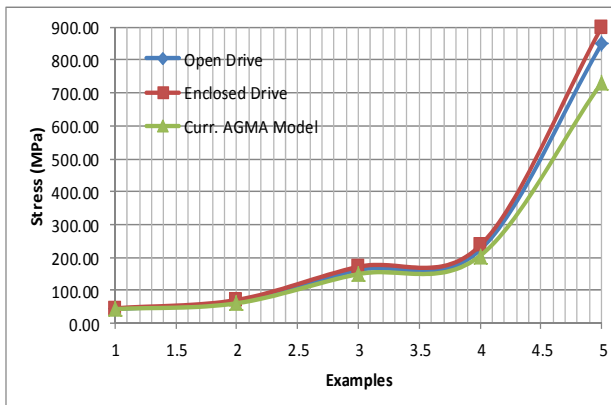


Fig. 12: New model and current AGMA model

From Table 6 and based on the range of mesh friction coefficient values studied, in an approximate but conservative estimate, it may be deduced that:

$$K_o \approx 1 + \zeta_m \quad (28)$$

Eqn. (28) summarizes the findings of this study in an approximate sense. It indicates that the influence of the mesh friction on the root bending stress of spur gears increases as the mesh friction coefficient value increases. This influence is marginal at low values such as may occur when an oil film is sustained in the gear mesh but grows and become more significant as boundary and dry friction lubrication regimes prevail.

Because mesh friction can only be estimated after a gearset dimensions are established and a lubricant is chosen, Eq. (28) is not helpful for initial sizing of spur gears. Hence it becomes necessary to approximate Eq. (24) with Eq. (25), especially during initial sizing (please see Eq. (A2) and Eq. (A3) in Appendix A1). This may be done by slightly increasing the nominal transmitted force. The increase can be achieved by defining a friction load factor with a value greater than

unity assigned and incorporated as a component in the service load factor. Such a factor can also accommodate miscellaneous effects of lubricant viscosity which partly determines lubrication effectiveness, and pitch line velocity influence on actual contact load in gear design. Since AGMA acknowledges the possible influence of surface roughness and friction on contact load in gears, this study enhances such AGMA notions because the friction load factor being suggested may be interpreted as being similar to AGMA surface finish factor.

11. CONCLUSIONS

A new revised Lewis bending stress capacity model is developed for spur gears and used to study the influence of frictional load in gear design. The mesh frictional load was resolved into tangential and radial components so that their contributions to spur gear root bending stress increases could be studied. While the increase in root bending stress by the tangential frictional load component could be directly predicted, that from the radial frictional load component was estimated by evaluating root bending stresses of five design examples. The analysis results indicate that the tangential frictional load component is the primary contributor in the increases in root bending stress. The radial frictional load component contributes marginally to root bending stress increases. It was demonstrated that the mesh friction load could increase gear root bending stress by up to about 6% in enclosed spur gear drives and 15% in open spur gear drives on the average. These increases can lead to over-stressing of gears; therefore a mesh friction should *always* be taken into account in root bending stress estimation as expressed approximately in Eq. (28). Since the mesh friction can only be estimated after a gearset is sized, a “friction load factor” (K_o) of 1.1 is suggested in this study for enclosed gear drives and 1.15 is suggested for open gear drives that is properly maintained for approximate analysis. It is commonly accepted that gear design is complicated and therefore, gear design procedures are not precise [25]. Hopefully, this study should help improve the accuracy of root bending stress estimation for cylindrical gears. It should be noted that very little damage, if any, is expected when an oil film is sustained between the gear teeth due to the low traction from the oil viscosity. Mild to severe damage may be expected when the gears operate in boundary friction regime or dry friction prevails due to the higher mesh friction coefficient arising from metal-to-metal contact.

APPENDIX A1: MESH FRICTION FOR CYLINDRICAL GEARS

The term “gear mesh friction” or simply “mesh friction” is used to characterize the frictional behavior occurring on the surfaces of a pair of gears in contact during operation. Frictional traction can arise from an oil film viscosity or from metal-to-metal contact during the steady-state or transient-state operation of a spur gearsets. An oil film exists in properly lubricated spur gears during normal or steady-state operation. At startup and shutdown or transient-state operation, boundary

lubrication is most likely and frictional load is inevitable. During normal operation in gears carrying extremely high specific load, the oil film may be squeezed out of the mesh or it may become difficult sustaining the oil film because of the heat generated and lubricant breakdown can occur. Consequently metallic contact between the gear teeth is inevitable and frictional load sets in. Mesh friction is important because frictional work leads to heat generation which reduces both the viscosity of gear lubricants and lubrication effectiveness. Lubricant breakdown can occur if the viscosity becomes too low, resulting in severe pitting or scoring of gear surfaces. The influence of frictional load on contact and bending stresses in gear meshes makes mesh friction a relevant concern in gear drives. However, very little damage, if any, is expected when an oil film is sustained between the gear teeth and mild to severe damage may be expected when the gears operate in boundary friction regime or dry friction prevails.

Gear mesh friction is complicated with contributions from sliding and rolling. However, pure rolling motion occurs only in the vicinity of the pitch point and a mixture of sliding and rolling motions predominate elsewhere [7]. Sliding friction is more significant in power loss than the rolling friction component. Higher peripheral speed facilitates the formation of an oil wedge in the contact area, resulting in lower frictional losses, [10]. A mesh friction model in wormsets where sliding motion is relatively high is of the form [26] given in Eq. (A1a). This is transformed into Eq. (A1b).

$$\zeta_m = \frac{A}{V_s^{0.25}} \quad A = \zeta_m V_s^{0.25} \quad (\text{A1})$$

Table A1 shows limited data on enclosed cylindrical gear sliding speed and mesh friction coefficient as reported by Petrov et al, [10, p. 114] in columns 1 and 2. Column 3 shows the average sliding velocity from column 1. Column 4 shows the value of constant “A” evaluated using Eq. (A1b) with the indicated average sliding speed in column 3 of the table. It is very encouraging that the values of “A” are remarkably close as indicated in column 4 of the table.

Table A1: Cylindrical Gear Mesh Friction Data

V_s range	ζ_m	V_s average	A estimate
0-3	0.100	1.5	0.110
3-5	0.063	4.0	0.089
5-10	0.060	7.5	0.099
10-20	0.050	15.0	0.098
Average			0.099

Based on the average value of “A” in Table A1, it is suggested that:

$$\zeta_m \approx \frac{0.10}{V_s^{0.25}} \quad 0.04 \leq \zeta_m \leq 0.10 \quad (\text{A2})$$

The average sliding speed in a cylindrical gear mesh may be estimated as given in Eq. (A3a) according to Maitra [11]. Eq. (A3b) gives the pitch or tangential velocity of the gear mesh for external gears. Note that Eq. (A3) can be used only after the gearset sizes are known.

$$V_s \approx 5V_t \left[\frac{1}{z_1} + \frac{1}{z_2} \right] \quad V_t = \frac{\pi d N}{60} \times 10^{-3} \quad (\text{A3})$$

It must be emphasized that Eq. (A2) gives an estimate of the average mesh friction coefficient, not the dynamic or instantaneous mesh friction coefficient.

When the mesh friction coefficient is estimated from Eq. (A2), the frictional load factor may be evaluated conservatively as:

$$K_o \approx 1 + \zeta_m \quad (\text{A4})$$

Eq. (A4) is useful during design verification or validation when the gearset is already sized.

Open gear drives operate in much harsher environments than enclosed gear drives and lubrication is not as good or as effective as in enclosed gears. Higher friction is therefore expected, since they operate mostly in boundary to dry friction regimes. For instance, the coefficient of friction in boundary lubrication is in the range of 0.05 to 0.15 [9]. Typically, the dry static friction coefficient for popular metallic gear materials appears to be in the range of 0.15 to 0.80 [27]. Dry kinetic friction coefficient is often at least 25% lower in value than dry static friction coefficient but may be as low as 50%. Lower values of kinetic friction coefficients are obtained when surfaces are lubricated with grease or oil.

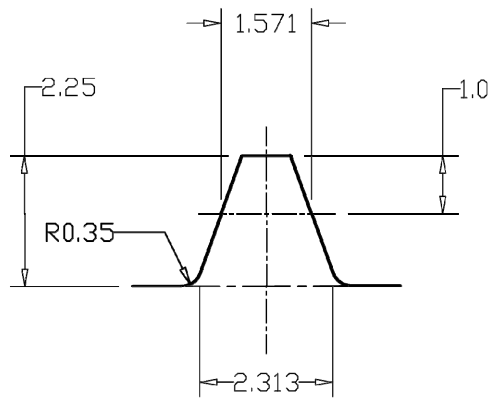
APPENDIX A2: BENDING MOMENT ARM FACTOR

It is observed in [28] that the bending stress form factor curves for different addendum correction factors converge to one point for a rack tooth. This indicates that the bending stress form factor for a rack is independent of the amount of addendum correction applied to the gear tooth. Now the rack tooth profile envelops all possible involute gear tooth shapes for a tooth standard and hence has a fixed tooth width at the root where the maximum tensile stress occurs. These reasons suggest that the bending moment arm factor λ_a may be estimated reliably by considering the basic rack profile of a gear tooth system.

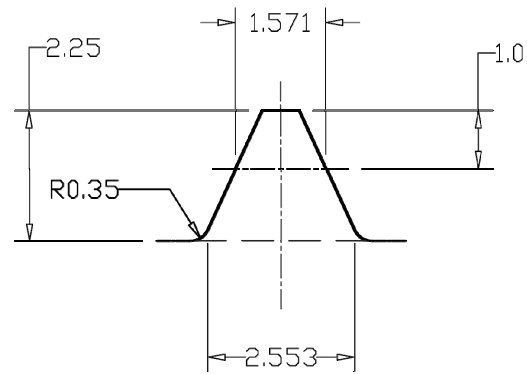
Fig. A1 shows the basic rack profile for 20° and 25° involute gear tooth standards. The fillet radius factor of 0.35 is a popular value in AGMA recommendations [29]. The root thickness is defined at the intersection of the fillet radius and the straight flank line of the rack tooth. A direct measurement of the root thickness which is equal to K for a module of 1 mm (Eq. 16b), can be made from these diagrams. Note that the fillet is tangential to both the straight flank line and the root or dedendum circle horizontal line shown as hidden line. Eq. (A5) is obtained from Eq. (16b).

$$\lambda_a = \frac{\kappa^2}{6Y'} \quad (\text{A5})$$

The value of Y' for a rack tooth is required in Eq. (A5) and was obtained from [30] and shown in column 2 of Table A2 for some popular involute gear tooth standards. The values of κ in the same table are obtained from Fig. A1. The fourth column in the table gives the values of λ_a for 20° and 25° involute gear tooth standards based on Eq. (4).



a) 20° tooth standard



b) 25° tooth standard

Fig. A1: Basic rack profile for 20° and 25° involute gear tooth standards

Table A2: Basic Rack Parameters for Bending Stress

Tooth Standard	Y^*	K	λ_a
20 std	0.47897	2.313	1.862
20 stub	0.54406	2.313	1.639
25 std	0.57139	2.553	1.901

*Values from [30]

ACKNOWLEDGEMENTS

This study was supported with funds from the College of Science, Engineering, and Technology (COSET) Research Fund and the University Faculty Development Fund of Texas Southern University, Houston, Texas. The authors are very grateful for this support.

NOMENCLATURE

1,2	subscript for pinion and gear respectively
A	a constant
b	nominal facewidth of gear (mm)
d	pitch diameter of pinion or gear (mm)
d_1	pitch diameter of pinion (mm)
f_n	resultant frictional force in transverse plane (N)
f_t	transverse frictional force (N)
f_r	radial frictional force (N)
F_r	nominal radial force (N)
F_t	nominal tangential force (N)
F_a	nominal axial force (N)
F_n	nominal normal contact force (N)
F_r'	effective radial force (N)
F_t'	effective tangential force (N)
k_1	contact length factor for pinion
k_2	contact length factor for gear
k_σ	effective normal stress concentration factors
k_τ	effective shear stress concentration factor
k_σ'	theoretical normal stress concentration factor
k_τ'	theoretical shear stress concentration factor
k_f	stress correction factor for root tensile stress
K_s	service load factor (nominal value)
K_s	service load factor (more accurate value)
K_{ss}	AGMA combined load factor
K_a	application or external overload factor
K_v	internal overload or dynamic factor.
K_m	mounting or mesh overload factor.
K_r	rim backup factor.

K_0	frictional load factor.
l_a	bending moment arm (mm)
m_t	transverse module (mm)
N	rotational speed of pinion or gear (rpm)
N_1	rotational speed of pinion (rpm)
P_1	power at pinion (kW)
q_σ	material normal stress notch sensitivity factor
q_τ	material shear stress notch sensitivity factor
r_n	pitch radius of pinion or gear in normal plane(mm)
t	root thickness (mm)
T_1	torque load at pinion (Nm)
V_s	average sliding speed
V_t	pitch tangential velocity (m/s)
Y'	Lewis bending stress form factor
z	number of teeth on a pinion or gear
z_1	number of teeth on pinion
z_2	number of teeth on gear
a_t	tangential friction load factor
a_r	radial friction load factor
λ_a	bending moment arm factor
κ	root thickness factor
\square_a	contact angle at tip of gear (deg.)
\square_t	transverse pressure angle (deg.)
σ_{bt}	root bending stress from tangential force (MPa)
σ_{cr}	compressive stress from radial force (MPa)
σ_b	combined normal stress at gear root (MPa)
σ_t	equivalent tensile stress at root of gear (MPa)
τ_s	direct shear stress at gear root (MPa)
\square_t	contact ratio in transverse plane
ζ_m	mesh friction coefficient

REFERENCES

- [1] Mott, R. L. (2004), *Machine Elements in Mechanical Design*, 4th ed. SI, Pearson Prentice Hall, New York.
- [2] Collins, J. A., Busby, H., Staab, G. H., (2010), *Mechanical Design of Machine Elements and Machines: A Failure Prevention Perspective*, 2nd ed., John Wiley and Sons, New York.
- [3] Bergseth, E. (2009), *Influence of Gear Surface Roughness, Lubricant Viscosity and Quality Level on ISO 6336 Calculation of Surface Durability*, Technical Report, Department of Machine Design, Royal Institute of Technology, Stockholm, <https://>

- [//www.diva-portal.org/smash/get/diva2:489751/FULLTEXT01.pdf](http://www.diva-portal.org/smash/get/diva2:489751/FULLTEXT01.pdf) (Accessed 8-20-19)
- [4] Schmid, S. R., Hamrock, B. J. and Jacobson, B. O., (2014), *Fundamentals of Machine Elements*, 3rd ed., CRC Press, New York.
- [5] Bommisetty, V. S. N. K., (2012), *Finite Element Analysis of Spur Gear Set*, Masters' Thesis, Mechanical engineering Department, Cleveland State University.
- [6] Kawalec, A., Wiktor, J., Ceglarek, D., (2006), *Comparative Analysis of Tooth-Root Strength Using ISO and AGMA Standards in Spur and Helical Gears with FEM-bases Verification*, Journal of Mechanical Design, Vol. 128, pp. 1141 – 1158.
- [7] Budynas, R. G. and Nisbett, J. K., (2010), *Shigley's Mechanical Engineering Design*, 9th ed., McGraw Hill Education.
- [8] Dobrovolsky, Zablonsky, K., Mak, S., Radchik, A., and Erlikh, L. *Machine Elements*, Foreign Language Pub. House, Moscow. (1965).
- [9] Shigley, J. E and Mischke, C. R. (Chief Editors), (1996), *Standard Handbook of Machine Design*, McGraw-Hill, New York.
- [10] Petrov, M., Chernilevsky, D., Berezovsky, Y. (1988), *Machine Design*, MIR, Moscow.
- [11] Maitra, G. M., (2013), *Fundamentals of Toothed Gearing: Handbook of Gear Design*, 2nd ed., McGraw Hill, New Delhi.
- [12] MITCal, *Involute Gearing-Theory*, www.mitcalc.com/doc/gear1/help/en/gear_theory.htm (Accessed 9-5-19)
- [13] Skakoon, J. G., *The Elements of Mechanical Design*, ASME Press, New York, 2008, p. 35
- [14] Skakoon, J. G., *Detail Mechanical Design*, ASME Press, New York, 2000, p. 122
- [15] Norton, R. L. (2000), *Machine Design: An Integrated Approach*, Prentice-Hall, Upper Saddle River, New Jersey.
- [16] Li, Z., and Mao, K., [2013], *Frictional Effects on Gear Tooth Contact Analysis*, *Advances in Tribology*, <http://dx.doi.org/10.1155/2013/181048>.
- [17] Eng, J., Karuppanan, S., and Patil, S., [2018], *Frictional Stress Analysis of Spur Gear with Misalignments*, *Journal of Mechanical Engineering Sciences*, Vol. 12, Iss. 2, pp. 3566 – 3580, DOI: <http://doi.org/10.15282/jmes.12.2.2018.4.0316>.
- [18] *Design for Strength, Lewis Bending Equation*, <https://images.search.yahoo.com/yhs/search> (Accessed 9-6-19)
- [19] *Stress Concentration Factors and Notch Sensitivity* https://moodle.ariel.ac.il/pluginfile.php/456050/mod_resource/content/0/Stress-concentration.pdf
- [20] Osakue, E. E. and Anetor, L., *Design Sizing Of Cylindrical Worm Gearsets*, *FME Transactions Journal*, 2019, **Accepted**.
- [21] Kragelskii, I. V. (1965), *Friction and Wear*, Butterworths, London, p. 1.
- [22] AGMA 2001-D04, *Fundamental Rating Factors and Calculation Methods for Involute Spur and Helical Gear Teeth*: <http://wp.kntu.ac.ir/avgari/AGMA%202001-D04.pdf>
- [23] Childs, P. R. N., *Mechanical Design Engineering Handbook*, Butterworth-Heinemann, Elsevier, 2014.
- [24] Edward E. Osakue, (2016), *Simplified Spur Gear Design*, Proceedings of International Mechanical Engineering Congress and Exposition 2016 IMECE, Paper Number IMECE2016-65426, November 11-17, Phoenix Arizona, USA.
- [25] *Introduction and Perspectives*, <https://www.asminternational.org/documents/>
- [26] RoyMech RoyMech, *Helical Gears*: http://www.roy-mech.co.uk/Useful_Tables/Drive/Helical_Gears.html
- [27] *Friction and Friction Coefficients*, https://www.engineeringtoolbox.com/friction-coefficients-d_778.html (2-16-19)
- [28] KHK https://khkgears.net/new/gear_knowledge/gear_technical_reference/bending-strength-of-spur-and-helical-gears.html
- [29] Juvinall, R. C. and Marshek, K. M. (2017), *Juvinall's Fundamentals of Machine Component Design*, S.I. Version, Wiley, Singapore.
- [30] Gopinath, K., Mayuram, M. M., *Machine Design II, Module 2 – Gears, Lecture 7 - Spur Gear Design*
- [31] https://nptel.ac.in/courses/112106137/pdf/2_7.pdf (8-13-19)

**ПАРАМЕТАРСКА АНАЛИЗА УТИЦАЈА
ОПТЕРЕЋЕЊА ОД ТРЕЊА
КОД ОТПОРНОСТИ НА САВИЈАЊЕ
ЦИЛИНДРИЧНИХ ЗУПЧАНИКА**

Е.Е.Осакуе, Л.Анетор, К.Харис

Приказан је модификовани Луисов модел капацитета напрезања услед замарања савијањем који је примењен у изучавању утицаја трења при спрезању на напон у корену зуба. Изворна Луисова формула је коришћена али су извршене модификације код динамичког оптерећења, смицајног напона и трења при спрезању код пројектовања цилиндричних зупчаника. Утврђено је да трење при спрезању може да повећа савојни напон до 6% код затворених зупчаника под претпоставком да је коефицијент трења услед спрезања 0,07. Повећање од 15% код напона у корену зупца може да настане код отворених зупчаника, када је коефицијент трења услед спрезања 0,15 што представља вредност која се сматра репрезентативном за правилно одржавање отворених зупчаника. Да би се објаснио утицај оптерећења од трења при спрезању и других фактора који утичу на трење од спрезања, предлаже се да вредност фактора оптерећења услед трења буде 1,1 за израчунавање оптерећења код затворених и 1,5 код отворених зупчаника.